sation, including SDC-2, SDC-3, DPY-26, DPY-27, MIX-1, and presumably DPY-28. These proteins colocalize over the X chromosomes, but it is not yet known if SDC-2 and SDC-3 directly contact the DPY-MIX protein complex. Antibodies to SDC-2 show that the protein remains associated with the X chromosomes even when other dosage compensation factors such as SDC-3 are defective (*6*). In contrast, SDC-2 binding to the *her-1* regulatory region is disrupted in the sex determination–specific *sdc-3*(Tra) mutants, which are defective in *her-1* repression. Therefore, the regulatory region of *her-1* might contain composite elements that can only stably bind SDC-2 and SDC-3 in concert. The density of regulatory elements recognized by SDC-2 and SDC-3 could also play a role in the stable arrangement of binding factors.

An exciting next phase of this work will undoubtedly address how SDC-2 mediates chromosome-wide recognition to assemble the dosage compensation machinery on the X. Although recognition of the *her-1* regulatory regions might be expected to occur by conventional DNA sequence-specific binding, it will be interesting to discover whether recognition of the X chromosome is less conventional. Dosage compensation in mammals, which occurs by X inactivation, is dependent on the cis-expression of a large noncoding RNA (Xist) rather than on DNA target sequences themselves, as inactivation can occur on autosomes that express multimers of Xist transgenes (*13*). Dosage compensation in *Drosophila* occurs by up-regulation of transcription in males and segments of the X retain dosage compensation when moved to autosomes, yet the identification of cis-acting sequences has been elusive (*5*). With SDC-2 and the complete sequence of the *C. elegans* genome in hand, one can envision a golden opportunity for understanding at least one way in which such a dramatic, chromosome-wide recognition mechanism has evolved.

References

1. P.-T. Chuang, D. G. Albertson, B. J. Meyer, *Cell* **79**, 459 (1994).
2. J. D. Lieb, E. E. Capowski, P. Meneely, B. J. Meyer, *Science* **274**, 1732 (1996).
3. J. D. Lieb, M. R. Albrecht, P.-T. Chuang, B. J. Meyer, *Cell* **92**, 265 (1998).
4. T. Hirano, R. Kobayashi, M. Hirano, *ibid.* **89**, 511 (1997).
5. T. W. Cline and B. J. Meyer, *Annu. Rev. Genet.* **30**, 637 (1996).
6. H. E. Dawes *et al.*, *Science* **284**, 1800 (1999).
7. C. Nusbaum and B. J. Meyer, *Genetics* **122**, 579 (1989).
8. L. M. Miller, J. D. Plenefisch, L. P. Casson, B. J. Meyer, *Cell* **55**, 167 (1988).
9. I. Carmi, J. B. Kopczynski, B. J. Meyer, *Nature* **396**, 168 (1998).
10. L. DeLong, J. D. Plenefisch, R. D. Klein, B. J. Meyer, *Genetics* **133**, 875 (1993).
11. T. L. Davis and B. J. Meyer, *Development* **124**, 1019-1031 (1997).
12. R. D. Klein and B. J. Meyer, *Cell* **72**, 349 (1993).
13. J. T. Lee and R. Jaenisch, *Curr. Opin. Genet. Dev.* **7**, 274 (1997).

PERSPECTIVES: MANTLE GEOCHEMISTRY

A Lesson from Ceramics

Alexandra Navrotsky

Understanding the properties of mantle materials is a great challenge, because reproducing the high pressures and temperatures of the mantle while performing detailed measurements on model materials is extremely difficult. The lower mantle is believed to be dominated by $MgSiO_3$-rich minerals with a perovskite structure, a compact structure often adopted by oxides containing two different cations of moderately different sizes. Minor elements such as calcium, aluminum, iron, and hydrogen as part of water or hydroxyl groups, affect the stability and properties of these minerals (*1–7*). However, many of the physical properties of $MgSiO_3$ perovskites under mantle conditions, such as defect mobility, ionic transport, and flow properties, remain poorly understood, and this hampers our understanding of fundamental mantle processes.

Enhanced online at www.sciencemag.org/cgi/content/full/284/5421/1788

In contrast to the silicate perovskites, ceramic perovskites have been studied extensively for fuel cell applications (*8–11*). Physical measurements under rigorously controlled conditions on these ceramic materials have yielded data essential to gaining quantitative understanding of defect equilibria and transport. As I will show below, these materials, which are ionic conductors when dry and fast proton conductors when wet, are useful analogs for mantle perovskites.

The tetravalent B cations in the ceramic $A^{2+}B^{4+}O_3$ perovskites may be Ti, Zr, Ce, or Sn. At atmospheric pressure the divalent A cations are limited to Ca, Sr, and Ba, but at high pressures Mn, Fe, and Mg may also be incorporated (*12*). Trivalent rare earth elements (M = Y, Yb, Nd, Gd) may substitute tetravalent ions, resulting in a doped series $A^{2+}(B^{4+}_{1-x}M_x)O_{3-0.5x}$ in which the diminished positive charge is compensated by oxygen vacancies (*8*). At high temperatures, these ceramic perovskites are oxide ion conductors or mixed ionic-electronic conductors (*8*).

The rare-earth–doped ceramic perovskites readily absorb water (*8–11*). Hydroxyl groups fill oxygen vacancies, creating mobile protons. The hydrogen bonds are relatively weak (*9*), and the structure relaxes around the defects (*9, 13, 14*). At low temperature, hydrogen is the mobile species, but above 750 K the proton and hydrogen mobilities are similar (*8–11*). Crystallographic studies show only minor changes in atomic positions with rare earth element doping (*15, 16*).

In the ceramic perovskites, defect equilibria are dominated by the following substitutions:

$$2B^{4+}_B = 2M^{3+}_B + V_O \quad (1)$$

$$V_O + O^{2-}_O + H_2O = 2OH^-_O \quad (2)$$

where subscript B denotes sites occupied by tetravalent B atoms in the original structure and subscript O denotes oxygen sites. Equation 1 creates oxygen vacancies, V_O, and Eq. 2 fills them. Equation 1 is most favored, and the trivalent ion solubility greatest, for the smallest size difference between the rare earth and tetravalent ion. The very strong relaxation of the neighboring oxygen atoms around each defect appears to compensate electrostatic and size mismatch locally and prevent long-range order. Hydration according to Eq. 2 is strongly exothermic by 100 to 170 kJ per mole of water, becoming more exothermic with increasing B-cation size for a given divalent cation. Proton mobility is favored by dense structures and short oxygen-oxygen distances.

These insights into the defect chemistry of ceramic perovskites can now be used to develop conceptual models for the behavior of $MgSiO_3$ under mantle conditions. Incorporation of trivalent species such as aluminum or ferric iron into $MgSiO_3$ perovskite can follow two competing mechanisms (*17*): vacancy formation according to Eq. 1 or coupled substitution of two trivalent ions for silicon and magnesium according to

$$Mg^{2+}_A + Si^{4+}_B = M^{3+}_A + M^{3+}_B \quad (3)$$

Atomistic simulations suggest that, at low pressure, oxygen vacancy formation (Eq. 1) is favorable for Al, whereas coupled substitution on B and A sites (Eq. 3) is favorable for Fe^{3+} (*4*). The latter is supported by experiment (*3*). The calculations sug-

The author is at the Thermochemistry Facility, Department of Chemical Engineering and Materials Science, University of California, Davis, CA 95616, USA. E-mail: anavrotsky@ucdavis.edu

gest that vacancy-free substitution may also become favorable above 30 GPa for Al because of the volume increase upon vacancy formation. This would suggest that Eq. 3 is the dominant defect formation mechanism in mantle perovskite.

However, these considerations neglect the fact that $MgSiO_3$ perovskite coexists with other mineral phases in the lower mantle. The defect equilibria must depend on which other phases are buffering the perovskite, and on whether the perovskite departs from ABO_3 stoichiometry. Silicate perovskite coexisting with a silica-rich phase (stishovite) must have a different equilibrium distribution of defects than perovskite coexisting with an MgO-rich phase (magnesiowustite).

To date, all experiments and simulations have been confined to the $MgSiO_3$-Al_2O_3 compositional series or join (see the figure). In contrast, perovskite in the mantle exists in a bulk rock composition approximately represented by the ellipse in the figure, with excess MgO potentially favoring the substitution along the $MgSiO_3$-$MgAlO_{2.5}$ join, which enriches the perovskite in Mg relative to Si. We have little hard data for understanding how this affects defect properties, but some general considerations can be made on the basis of the available data and by analogy with the ceramic perovskites.

For a given bulk composition, the phase assemblage formed following Eq. 1 would contain more perovskite and less magnesiowustite than that formed according to Eq. 3, because in Eq. 1 no Mg is replaced in the perovskite structure. Which assemblage is denser depends critically on the thermal expansivity, compressibility, and molar volume of aluminous perovskite formed by each substitution mechanism. These parameters are not known well enough to say more than that the two assemblages differ little in volume. Thus, defect substitution involving excess magnesium and oxygen vacancies is not precluded at high pressure from volumetric arguments if one considers the complete phase assemblage rather than the perovskite alone. On the other hand, neither is it proven.

Possible evidence for a vacancy-coupled substitution of aluminum or iron (or both) according to Eq. 1 includes the detection of excess SiO_2 (stishovite) in perovskite synthesized along the $MgSiO_3$-Al_2O_3 join (*18, 19*), implying that the aluminous perovskite formed is somewhat MgO-rich and thus indicating that oxygen vacancy formation following Eq. 1 occurs. The surprisingly large effect of as little as 5% aluminum substitution in softening the elastic properties, thermal expansivity, and Anderson-Gruneisen parameter of $MgSiO_3$ perovskite (*20*) may also support the presence of oxygen vacancies. Finally, when 2.89% Al_2O_3 is dissolved in a perovskite with a small iron content, the electrical conductivity increases by a factor of 3.5, as does the ferric iron concentration (*1*).

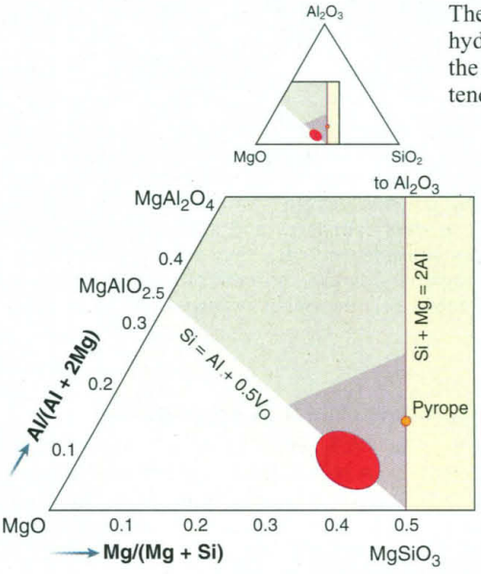

Part of the MgO-SiO_2-Al_2O_3 system showing the possible perovskite stability field. The $MgSiO_3$-Al_2O_3 and $MgSiO_3$-$MgAlO_{2.5}$ joins are likely limits to the substitution of aluminum in perovskite. The shaded area schematically shows the region where a single-phase perovskite could form. The filled ellipse represents likely mantle compositions. The dot represents the ideal composition of the garnet pyrope.

This may be attributed to the charge-balanced ionic substitution of incorporated ferric iron and aluminum, excess magnesium, and oxygen vacancies.

Thus, although the evidence is still scarce, excess MgO and oxygen vacancy substitution mechanisms may well play a role in silicate perovskite. The proton-conducting ceramic perovskites may then serve as a model for the role of water in aluminous silicate perovskites. In the ceramic proton conductors, hydration of vacant oxygen sites by Eq. 2 is energetically favorable. The lower basicity of Mg would make the hydration enthalpy less exothermic than for Sr and Ba. High temperature opposes hydration, but high pressure favors it. The high density and short O-O distance in $MgSiO_3$ would favor hydration and proton migration. The incorporation of water is volumetrically favorable, reflecting the high density of the perovskite with vacancies filled by hydroxyl groups. A quantitative assessment of these factors is not possible without experimental data, but the coupled substitution of water and aluminum must certainly be considered.

Further, ceramic perovskites are thermodynamically stabilized by hydration and therefore may incorporate significantly more trivalent ions under hydrous than under anhydrous conditions. Analogously, significantly more aluminum and other trivalent ions could be incorporated into silicate perovskite in the presence of water. The coupling of Eqs. 1 and 2 suggests that hydrated perovskite-related phases along the $MgSiO_3$-$MgAlO_2(OH)$ join could extend further than in the anhydrous system.

What do these considerations mean in practice for mantle processes? A cold subducting slab may bring hydrous phases from Earth's crust through the transition zone into the lower mantle (*21*). As the slab warms, dense hydrous magnesium silicates dehydrate. If the perovskite phase surrounding the slab contains even small amounts of oxygen vacancies, they could absorb the water from the slab, which could then be distributed rapidly throughout the surrounding mantle by proton migration. The strong relaxation around the defects and the ease of proton hopping may lead to considerable softening, with larger anharmonicity, larger thermal expansion, lower bulk modulus, and easier plastic flow than if there were no oxygen vacancies that could be hydrated.

The analogy with ceramic perovskites suggests a very rich high-pressure chemistry of both hydrated and anhydrous perovskites in silicates of geologically relevant compositions, with wide ranging implications for their physical and chemical properties. Experimental and theoretical studies along the $MgSiO_3$-$MgAlO_{2.5}$ join series are being performed to test the validity of this analogy.

References and Notes

1. Y. Xu *et al.*, *Science* **282**, 922 (1998).
2. B. J. Wood and D. C. Rubie, *ibid.* **273**, 1522 (1996).
3. C. McCammon, *Nature* **387**, 694 (1997).
4. N. C. Richmond and J. P. Brodholt, *Am. Mineral.* **83**, 947 (1998).
5. D. Andrault *et al.*, *ibid.*, p. 1045.
6. S. E. Kesson *et al.*, *Earth Planet. Sci. Lett.* **134**, 187 (1995).
7. C. Meade *et al.*, *Science* **264**, 1558 (1994).
8. K. D. Kreuer, *Solid State Ionics* **97**, 1 (1997).
9. _____, *Chem. Mater.* **8**, 810 (1996).
10. T. Norby, *Solid State Ionics* **40**, 857 (1990).
11. A. S. Nowick and Y. Du, *ibid.* **77**, 137 (1995).
12. A. Navrotsky, *Chem. Mater.* **10**, 2787 (1998).
13. M. Pionke *et al.*, *Solid State Ionics* **97**, 497 (1997).
14. J. L. Labrincha *et al.*, *ibid.* **61**, 71 (1993).
15. J. Ranlov and K. Nielson, *J. Mater. Chem.* **4**, 867 (1994).
16. K. S. Knight *et al.*, *ibid.* **2**, 709 (1992).
17. L. M. Hirsch and T. J. Shankland, *Geophys. Res. Lett.* **18**, 1305 (1991).
18. E. Ito *et al.*, *ibid.* **25**, 821 (1998).
19. A. Kubo *et al.*, *Rev. High Press. Sci. Technol.* **7**, 122 (1998).
20. J. Zhang and D. J. Weidner, *Eos* **79**, F861 (1998).
21. K. Bose and A. Navrotsky, *J. Geophys. Res.* **103**, 9713 (1998).

22. Supported by CHiPR, the Center for High Pressure Research, an NSF Science and Technology Center.